

DNA Bending by GCN4 Mutants Bearing Cationic Residues<sup>†</sup>J. K. Strauss-Soukup<sup>‡,§</sup> and L. J. Maher, III<sup>\*,§</sup>

Department of Biochemistry and Molecular Biology and Eppley Institute for Research in Cancer and Allied Diseases, University of Nebraska Medical Center, Omaha, Nebraska 68198, and Department of Biochemistry and Molecular Biology, Mayo Foundation, Rochester, Minnesota 55905

Received January 29, 1997; Revised Manuscript Received May 13, 1997<sup>®</sup>

**ABSTRACT:** Transcription activation is thought to require DNA bending to promote the interaction of upstream activators and the basal transcription machinery. Previous experiments have shown that some members of the bZIP family of DNA binding proteins bend DNA, while others do not. We are exploring the possibility that electrostatic effects play a role in these differences. The yeast bZIP transcription factor GCN4 does not induce DNA bending *in vitro*. Substitution of basic residues for three neutral amino acids of GCN4 confers the ability to bend DNA. This result is consistent with a model of induced DNA bending wherein excess positive charge in proximity to one face of the double helix neutralizes local phosphate diester anions resulting in a laterally asymmetric charge distribution along the DNA. Previous data suggest that such an unbalanced charge distribution results in collapse of the DNA toward the neutralized surface. Interpretations of the present data are discussed. Our result supports the hypothesis that electrostatic interactions can play a key role in DNA bending by bZIP proteins.

DNA bending presumably plays a significant role in the functional architecture of all promoters (Perez-Martin & Espinosa, 1993; Perez-Martin et al., 1994; Travers, 1992; Zinkel & Crothers, 1991). Multiple transcription factors are thought to bind and reconfigure the duplex DNA, allowing initiation and activation of transcription by RNA polymerase (Giese et al., 1995; Robertson et al., 1995; Thanos & Maniatis, 1995). Contacts between transcription factors and the basal transcription machinery are critical in this process. The interactions between these distant proteins are thought to be mediated by DNA bending (Bracco et al., 1989; Gartenberg & Crothers, 1988; Gartenberg & Crothers, 1991; McAllister & Achberger, 1989; Zinkel & Crothers, 1987; Zinkel & Crothers, 1991).

A variety of proteins have been shown to bend DNA *in vitro*. For example, the TATA binding protein (TBP)<sup>1</sup> is observed to bend duplex DNA by ~90° in solution (Parkhurst et al., 1996; Starr et al., 1995) and in crystals (Kim et al., 1993a,b). Some bZIP proteins, such as the Jun-Fos heterodimer, appear to induce DNA bending (Kerppola & Curran, 1991a,b). bZIP proteins dimerize and bind DNA through conserved basic and leucine zipper regions (Figure 1; Landschulz et al., 1988; McKnight, 1991). The leucine zipper stabilizes a coiled coil of  $\alpha$  helices common to the

many combinations of homo- and heterodimers observed among bZIP family members. The basic region is a continuous  $\alpha$  helix that contacts base pairs within the major groove of the DNA recognition site (e.g., 5'-ATGACTCAT for AP-1; Jun-Fos heterodimer). There is evidence that the basic region attains this structure only upon DNA binding (O'Neil et al., 1991).

Interestingly, different bZIP homo- and heterodimers have been found to bend DNA to different extents and in different directions (Table 1; Kerppola & Curran, 1993). Three amino acids positioned just N-terminal to the basic region may be important (Figure 1 and Table 1). It has been noted that the presence of basic residues in these positions correlates with DNA bending away from the leucine zipper in the resulting complexes (Kerppola & Curran, 1993; Paolella et al., 1994). This observation suggests that these cationic amino acids contact one face of the DNA and interact with the negatively charged phosphate diester backbone. In light of our previous studies on DNA bending by asymmetric phosphate neutralization (Strauss & Maher, 1994; Strauss et al., 1996a,b), we have been intrigued by the role of these basic residues in DNA bending by bZIP proteins.

A testable implication of the data in Table 1 is that substitution of three basic amino acids might convert GCN4 (a yeast bZIP protein that does not induce DNA bending; Gartenberg et al., 1990) into a DNA bending protein. We describe experiments that confirm this hypothesis.

## EXPERIMENTAL PROCEDURES

**Oligonucleotides.** Oligonucleotides were synthesized on an ABI model 380B instrument using standard procedures. Oligonucleotides were cleaved and deprotected in hot ammonia and purified by denaturing polyacrylamide gel electrophoresis, eluted from gel slices, and desalted using C<sub>18</sub> reverse-phase cartridges. Oligonucleotide concentrations were determined at 260 nm using molar extinction coefficients (M<sup>-1</sup> cm<sup>-1</sup>) of 15 400 (A), 11 700 (G), 7300 (C), and 8800 (T) assuming no hypochromicity.

<sup>†</sup> Supported by the Mayo Foundation and NIH Grants GM47814 and GM54411 to L.J.M. and a University of Nebraska Medical Center Regents Fellowship to J.K.S.-S. L.J.M. is a Harold W. Siebens Research Scholar.

\* Author to whom correspondence should be addressed.

<sup>‡</sup> University of Nebraska Medical Center.

<sup>§</sup> Mayo Foundation.

<sup>®</sup> Abstract published in *Advance ACS Abstracts*, July 15, 1997.

<sup>1</sup> Abbreviations: bp, base pair(s); DTT, dithiothreitol; EDTA, ethylenediaminetetraacetic acid; Tris-HCl, 2-amino-2-(hydroxymethyl)-1,3-propanediol hydrochloride; IPTG, isopropyl  $\beta$ -D-thiogalactopyranoside; bZIP, basic zipper; TBP, TATA-box binding protein; TBE, Tris-borate-EDTA; TBS-T, Tris-buffered saline-Tween 20; SDS, sodium dodecyl sulfate; NP-40, tergitol NP-40 (nonylphenoxypolyethoxyethanol); P, proline; A, alanine; K, lysine; R, arginine; M, methionine; S, serine; T, threonine; G, glycine; Q, glutamine; L, leucine; E, glutamic acid.

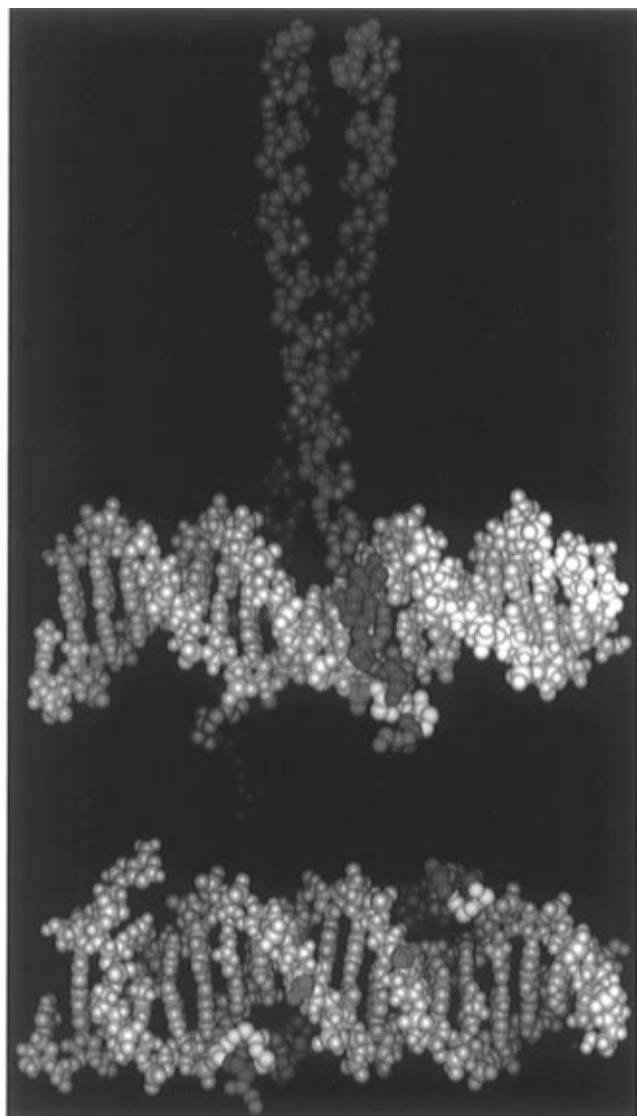


FIGURE 1: Side and bottom views of a GCN4 homodimer complex with duplex DNA containing an AP-1 site (Ellenberger et al., 1992). DNA and protein are in gray and blue, respectively. Basic amino acids of GCN4 are shown in red. The three amino acids that are mutated in this study are indicated in yellow. The sites of nearest putative phosphate contacts are indicated in green. Molecular modeling was performed using Insight II (version 95.5) software obtained from Molecular Simulation Inc. (San Diego, CA) and a Silicon Graphics Indigo II workstation.

**Plasmids.** Plasmid pJ013 (previously termed pLc28-bZIP; Suckow et al., 1993b) encodes the basic and zipper regions of GCN4 (amino acids 226–281). Plasmids pJT170-2 through pJT170-9 (Thompson & Landy, 1988) were used as standards in phasing analyses. This series of plasmids contains increasing numbers of phased A<sub>6</sub> tracts. Plasmids pDP-AP-1-21, -23, -26, -28, and -30 (Paolella et al., 1994) were used to generate phasing probes (see below). The GCN4(PAA→KRR) derivative was created by digesting pJ013 with *Nde*I and *Bss*HII. Oligonucleotides 5′-TATG<sub>2</sub>-CTAGCATGACTG<sub>2</sub>TG<sub>2</sub>ACAGCA<sub>3</sub>TG<sub>3</sub>TCG<sub>3</sub>ATA<sub>3</sub>-CGTCGT<sub>3</sub>A<sub>4</sub>CGTG-3′ and 5′-CGCGCACGT<sub>4</sub>A<sub>3</sub>CGACGT<sub>3</sub>-ATC<sub>3</sub>GAC<sub>3</sub>AT<sub>3</sub>GCTGTC<sub>2</sub>AC<sub>2</sub>AGTCATGCTAGC<sub>2</sub>A-3′ were annealed in a 1:1 ratio. This synthetic duplex was ligated between the *Nde*I and *Bss*HII sites of pJ013 to create plasmid pJ024. A plasmid encoding the GCN4(PAA→KKK) derivative was created by digesting pJ013 with *Nde*I and *Bss*HII. Oligonucleotides 5′-TATG<sub>2</sub>CTAGCATGACTG<sub>2</sub>TG<sub>2</sub>ACAG-

Table 1: Basic Residues Adjacent to the Conserved Basic Domains of bZIP Proteins Correlate with DNA Bending<sup>a</sup>

bZIP protein	amino acids at the amino end of the basic region <sup>b</sup>	net charge of tripeptide	bend toward DNA minor groove <sup>c</sup>
FOS	<u>KRR</u>	+3	++
FRA1	<u>RRR</u>	+3	+
FRA2	<u>KRR</u>	+3	+
ATF2	<u>KRR</u>	+3	+
JUN	<u>KAE</u>	0	–
CREB	<u>KRE</u>	+1	–
ATF1	<u>KRE</u>	+1	–
ZTA	<u>ELE</u>	–2	–
GCN4	PAA	0	–

<sup>a</sup> Bending data were interpreted according to the independent DNA bends model (Kerppola & Curran, 1991a). <sup>b</sup> The indicated tripeptide corresponds to residues 227–229 of GCN4 (Ellenberger et al., 1992). Basic amino acids are underlined. <sup>c</sup> Kerppola and Curran, 1993; (++) indicates a bend angle >20° toward minor groove, (+) indicates a bend angle <20° toward minor groove, and (–) indicates a bend angle toward the major groove.

CA<sub>3</sub>TG<sub>3</sub>TCG<sub>3</sub>ATA<sub>9</sub>T<sub>2</sub>A<sub>4</sub>CGTG-3′ and 5′-CGCGCACGT<sub>4</sub>A<sub>2</sub>-T<sub>9</sub>ATC<sub>3</sub>GAC<sub>3</sub>AT<sub>3</sub>GCTGTC<sub>2</sub>AC<sub>2</sub>AGTCATGCTAGC<sub>2</sub>A-3′ were annealed in a 1:1 ratio. This synthetic duplex was ligated between the *Nde*I and *Bss*HII sites of pJ013 to create plasmid pJ145.

**Bacterial Extracts Containing Recombinant GCN4 Derivatives.** Plasmid pJ013 expressing the bZIP domain of GCN4, plasmid pJ024 expressing the mutated GCN4-(PAA→KRR) derivative, or plasmid pJ145 expressing the mutated GCN4(PAA→KKK) derivative was transformed into *Escherichia coli* BL21(DE3) cells. Cultures were grown to log phase ( $A_{600} \sim 0.6$ ) at 37 °C, IPTG was added to a final concentration of 1 mM, and cells were grown an additional 3 h (Studier et al., 1990). Cells were harvested by centrifugation, and the cell pellet was resuspended in extraction buffer (200 mM Tris-HCl, pH 8.0, 10 mM MgCl<sub>2</sub>, 1 mM EDTA, 7 mM β-mercaptoethanol) and sonicated (Fisher Scientific) on ice for 1 min at a setting of 10 W (Suckow et al., 1993a). After centrifugation for 30 min (4 °C, 12 000g), aliquots of the clarified supernatant were snap frozen and stored at –80 °C.

**Preparation of DNA Duplex Probes.** Probes for phasing analysis were prepared by PCR amplification of 437–446-bp fragments containing an AP-1 site in various phasings relative to an array of three intrinsically bent A<sub>5</sub> tracts. Primers 5′-GCA<sub>2</sub>GCT<sub>2</sub>GCG<sub>2</sub>C<sub>2</sub>GC<sub>3</sub>AT<sub>2</sub>AT<sub>2</sub>ATCATGACAT<sub>2</sub>A<sub>2</sub>C-3′ and 5′-G<sub>2</sub>TAC<sub>2</sub>GCTA<sub>2</sub>GCTCATAACAG<sub>2</sub>TGC<sub>2</sub>TG-3′ are complementary to regions within plasmids pDP-AP-1-21, -23, -26, -28, and -30 (Paolella et al., 1994) and were used for PCR amplification to generate duplex DNA probes containing the AP-1 site. The resulting phasing probes were designated AP-1-21, -23, -26, -28, and -30. PCR reactions (100 μL total) contained ~10 nM template DNA, 1 μM each of primer, 200 μM d(GAT)TP, 50 μM dCTP, 1.5 mM MgCl<sub>2</sub>, 50 mM KCl, 10 mM Tris-HCl (pH 8.3), 2 μL of [α-<sup>32</sup>P]dCTP (10 mCi/mL; 3000 Ci/mmol), and 100 units/mL Tth DNA polymerase (Epicentre Technologies). DNAs were amplified by 20 cycles consisting of incubation at 94 °C for 60 s, 50 °C for 75 s, and 72 °C for 120 s. Reactions were extracted with an equal volume of chloroform.

Pairs of curved DNA standards containing different numbers of phased A<sub>6</sub> tracts at either the center or the end

of each fragment were prepared by *NheI* and *BamHI* cleavage of plasmids pJT170-2 through pJT170-9 (Thompson & Landy, 1988). The resulting ~400-bp duplex DNA fragments were purified by nondenaturing polyacrylamide gel electrophoresis (5% acrylamide; 1× TBE), visualized by UV shadowing, excised, and eluted overnight at 37 °C with agitation in water. The eluant was extracted with an equal volume of phenol–chloroform (1:1 v/v), and duplex DNA was ethanol precipitated. Duplex DNA was radiolabeled using T4 DNA polymerase (New England Biolabs) and [ $\alpha$ - $^{32}$ P]dATP in the presence of 0.2 mM d(GTC)TPs (Deen et al., 1983).

**Western Blot Analysis.** Protein concentrations were determined using the Bio-Rad (Bradford) assay with detection at 595 nm. Ten micrograms of total protein from each extract was separated on 10–20% SDS–polyacrylamide gels in tricine buffer and transferred onto nitrocellulose. The membrane was blocked with an overnight incubation in 1% non-fat dry milk and TBS-T (10 mM Tris-HCl, pH 8.0, 150 mM NaCl, and 0.05% Tween 20), followed by successive incubations with anti-T7 tag mouse monoclonal antibody (1:10 000), anti-mouse fluorescein-linked antibody (1:100), and anti-fluorescein alkaline phosphatase conjugate (1:2500), all in TBS-T containing 1% non-fat dry milk. In the final step, alkaline phosphatase catalyzes the conversion of AttoPhos (JBL Scientific Inc.) to a product that fluoresces at 540–560 nm. Fluorescent detection was performed with a Storm 840 instrument (Molecular Dynamics Inc.).

**Electrophoretic Gel Mobility Shift Assays.** Binding reactions were performed by incubation of the indicated extract (5–10  $\mu$ L) with 1  $\mu$ L of radiolabeled, duplex DNA probes (AP-1-21, -23, -26, -28, or -30; see above) in a final reaction mixture containing phosphate-buffered saline (2.7 mM KCl, 137 mM NaCl, 4.3 mM Na<sub>2</sub>HPO<sub>4</sub>, and 1.4 mM KH<sub>2</sub>PO<sub>4</sub>, pH 7.3), 5% glycerol, 1 mM EDTA, 1 mM DTT, 0.05% NP-40, and 26–36  $\mu$ g/mL poly(dI·dC) as described by Paoletta et al. (1994). Binding reactions were incubated on ice for 10 min. Free and protein-bound DNA probes were resolved by nondenaturing 5% polyacrylamide gel electrophoresis (29:1 acrylamide:bisacrylamide) in 0.5× TBE buffer for 16 h at 4 °C (12 V·cm<sup>-1</sup>). Dried gels were analyzed by storage phosphor technology.

**Phasing Analysis Calculations.** Mobilities ( $\mu$ ) of free and bound DNA fragments were taken as the distance (mm) from the center of the electrophoresis well to the center of the band corresponding to free or protein-complexed DNA and were normalized to the average mobility of each set of probes to give relative mobility:

$$\mu_{\text{rel}} = \mu / \bar{\mu} \quad (1)$$

where  $\bar{\mu}$  corresponds to the average value of  $\mu$  for a set of phasing probes. Values of  $\mu_{\text{rel}}$  were then plotted against the phasing spacing (distance in bp between the center of the AP-1 site and the center of the A<sub>5</sub> tract array) for fitting to the phasing function:

$$\mu_{\text{rel}} = (A_{\text{PH}}/2) \{ \cos [2\pi(S - S_T)/P_{\text{PH}}] \} + 1 \quad (2)$$

where  $\mu_{\text{rel}}$  is the relative mobility of the free or protein-complexed DNA,  $S$  is the phasing spacer length,  $P_{\text{PH}}$  is the phasing period (set at 10.5 bp/turn),  $S_T$  is the trans spacer length (the length where the intrinsic and protein-induced

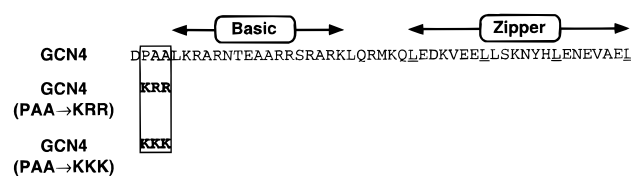


FIGURE 2: Amino acid sequences of the recombinant GCN4 derivatives studied. Leucines of the zipper heptad repeat are underlined. Both wild-type and mutant recombinant proteins also contain the N-terminal sequence MASMTGGQMQMR and the C-terminal sequence KKLESGQ.

bends are predicted to most nearly cancel giving maximal mobility), and  $A_{\text{PH}}$  is the amplitude of the phasing function (Kerppola, 1994). The value of  $A_{\text{PH}}$  is estimated by curve fitting and is related to the magnitude of the directed bend. Curve fitting was performed by the least squares method using KaleidaGraph software (Synergy Software Co.). The directed DNA bend angle,  $\alpha_B$ , is obtained using the relation:

$$\tan(k\alpha_B/2) = (A_{\text{PH}}/2)/\tan(k\alpha_C/2) \quad (3)$$

where  $\alpha_C$  is the reference bend angle magnitude (54° for three A<sub>5–6</sub> tracts) and  $k$  is empirically determined using the bending standard duplexes. To determine  $k$ , the mobilities of the bending standards are fit to the function:

$$A_{\text{CP}} = 1 - \cos(k\alpha/2) \quad (4)$$

where  $\alpha$  is the angle due to the A<sub>5–6</sub> tracts and  $A_{\text{CP}}$  is the amplitude of the circular permutation function reflecting the magnitude of the DNA distortion (Kerppola, 1994). The value  $A_{\text{CP}}$  is given by

$$A_{\text{CP}} = |(\mu_{\text{center}}/\mu_{\text{end}}) - 1| \quad (5)$$

where  $\mu_{\text{center}}$  and  $\mu_{\text{end}}$  are mobilities of circularly permuted DNA fragments where phased arrays of A<sub>6</sub> tracts are located at the center or end of the fragment, respectively (see lanes 1–4 of Figure 5A and lanes 11–17 of Figure 5B). The average value of  $k$  under the present electrophoretic conditions was 1.1.

## RESULTS

**Design of GCN4(PAA→KRR) and GCN4(PAA→KKK) Mutants.** Previous experiments have shown that the presence of basic amino acids adjacent to the conserved basic domains of bZIP proteins correlates with DNA bending toward the minor groove (away from the leucine zipper; Table 1). The yeast bZIP protein GCN4 contains the sequence PAA adjacent to the basic region and does not appreciably bend DNA in electrophoretic experiments (Gartenberg et al., 1990). We hypothesized that mutation of these neutral amino acids to the basic amino acids KRR (as found in Fos; Table 1 and Figure 2) or to KKK would induce DNA bending by GCN4 homodimers.

GCN4 mutant proteins were expressed at reduced levels in *E. coli* as assayed by Western blotting (Figure 3). GCN4 derivatives were expressed with an N-terminal T7 tag sequence that is recognized by the monoclonal T7 tag antibody. Chemifluorescence detection allowed for estimation of protein levels in Western blots. GCN4(PAA→KRR) was expressed at only ~7% of wild-type levels. GCN4(PAA→KKK) was expressed at ~36% of wild-type levels. Because we used crude bacterial lysates for gel mobility shift

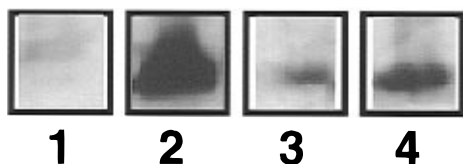


FIGURE 3: Western analysis. Western blot of crude protein extracts from *E. coli* BL21(DE3) cells expressing different proteins. Lane 1 contains extract from *E. coli* cells carrying expression vector alone, lane 2 contains extract of cells expressing the wild-type GCN4 derivative, lane 3 contains extract of cells expressing GCN4-(PAA→KRR), and lane 4 contains extract of cells expressing GCN4(PAA→KKK).

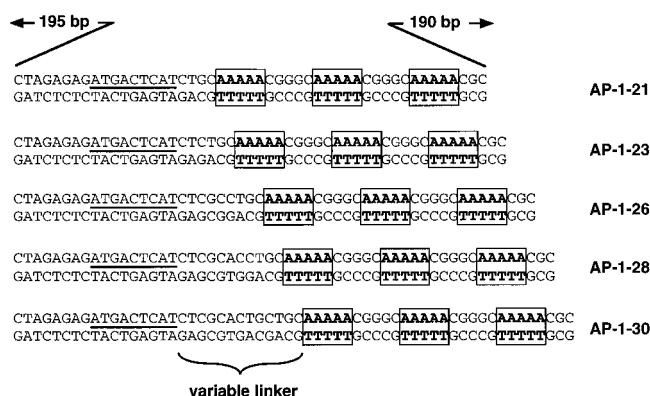


FIGURE 4: Phasing analysis probes used to study DNA bending by GCN4 derivatives. Probes used for phasing analysis contained an AP-1 site (underlined) separated by a variable number of bp from a 25-bp array of A<sub>5</sub> tracts (bold and boxed) that is intrinsically bent toward the minor groove by  $\sim 54^\circ$  (in a reference frame near the center of the central A<sub>5</sub> tract). Probe designations are shown at the right indicating the distance (bp) between the center of the AP-1 site and the center of the 25-bp A<sub>5</sub> tract array. Probes are 437–446 bp in length, and the AP-1 site is 203 bp from the left terminus of each probe.

experiments, differences in protein expression are reflected in different degrees of probe saturation.

*Phasing Analysis.* Changes in average DNA shape due to intrinsic curvature of the duplex or protein-induced bending were studied by electrophoretic mobility shift assays. Nondenaturing gel electrophoresis allows for detection of phase-dependent changes in electrophoretic mobility. These effects result when a DNA fragment containing a protein recognition sequence (e.g., the AP-1 site) also contains a reference sequence of defined curvature, in this case an array of A<sub>5</sub> tracts. Phasing analysis measures the overall DNA shape as the distance between these elements of curvature is altered (Kerppola, 1996; Kerppola & Curran, 1991a; Paolella et al., 1994; Zinkel & Crothers, 1987). This technique is sensitive and distinguishes directed bends from distortions that result from isotropic flexibility. Phasing analysis also allows for definition of the orientation of a directed bend relative to the intrinsic curvature present in the fragment.

The 437–446-bp phasing probes used to study DNA bending by GCN4 derivatives are shown in Figure 4. Only the sequences surrounding the AP-1 site and A<sub>5</sub> tract array are shown. The AP-1 site (ATGACTCAT) is separated from a 25-bp curved DNA element by a variable linker. The 25-bp curved sequence contains three A<sub>5</sub> tracts with an overall curvature of 54° toward the minor groove (in a reference frame taken to be 0.5 bp 3' to the central A of the central A<sub>5</sub> tract in the array). The five probes differ only in the length

of the variable linker that changes the phasing of the AP-1 site and A<sub>5</sub> tract array.

*AP-1 Phasing Probes Have Intrinsic Curvature.* Lanes 5–9 of Figure 5A depict mobilities of phasing probes incubated with *E. coli* extract lacking GCN4 peptides. The absence of any shifted complexes indicates that there are no endogenous *E. coli* proteins that bind to the phasing probes. Slight intrinsic probe curvature in or near the AP-1 site is implied by the different mobilities observed for the five phasings. An estimate of  $\sim 8^\circ$  intrinsic curvature toward the major groove at the AP-1 site was determined from the phasing analysis and the assumption that the center of the AP-1 site is the site of curvature (Figure 6; Table 2). However, the actual site of curvature cannot be determined from this study. Previous experiments with shorter phasing probes (164–173 bp) containing the sequences flanking the AP-1 site estimated the AP-1 site to be curved  $\sim 3^\circ$  toward the major groove (Paolella et al., 1994). The slight difference in these estimates may be attributable to the difference in length of the phasing probes. The longer phasing probes used in our study are thought to allow for more sensitive determination of bend angles (Kerppola, 1996).

**GCN4 Does Not Bend the AP-1 Site.** Binding reactions containing the AP-1 probes and extract containing wild type GCN4 protein (basic and zipper regions) resulted in complexes whose mobilities reflected the same DNA curvature pattern as was observed for the free probes (Figure 5A, compare lanes 5–9 with lanes 10–14). Analysis of these phasing data suggests a bend angle of  $\sim 6^\circ$  toward the major groove (Figure 6; Table 2). This value is comparable to the  $\sim 8^\circ$  intrinsic curvature measured for the unbound AP-1 site.

*GCN4(PAA→KRR) and GCN4(PAA→KKK) Induce DNA Bending.* Binding reactions containing the AP-1 probes and bacterial extract containing recombinant GCN4(PAA→KRR) protein or recombinant GCN4(PAA→KKK) protein produced complexes whose mobilities suggested very different DNA curvatures than those measured for free probes or wild-type GCN4–DNA complexes (Figure 5A, compare mobility patterns in lanes 5–14 with lanes 15–19; Figure 5B, compare mobility patterns in lanes 1–5 with lanes 6–10). The mobility patterns for GCN4(PAA→KRR)–DNA complexes and GCN4(PAA→KKK)–DNA complexes indicate induced bending in the opposite direction from the intrinsic curvature of the AP-1 site (Figure 6; Table 2). For both mutants with cationic residues, the induced bend angle amounted to  $\sim 20^\circ$  toward the minor groove ( $\sim 15^\circ$  toward the minor groove in addition to reversal of the  $\sim 5^\circ$  of curvature toward the major groove in the wild-type GCN4–DNA complex). Thus, mutation of three amino acids endows the GCN4 mutants with substantial DNA bending characteristics.

## DISCUSSION

Numerous techniques have been employed to measure DNA bending by bZIP proteins such as AP-1 (Jun+Fos; Hagerman, 1996; Kerppola, 1996; Kerppola & Curran, 1993; Sitlani & Crothers, 1996). Original work by Kerppola and Curran employed electrophoretic phasing analysis and indicated that these complexes bend DNA and that the orientations of DNA bending induced by Fos-Jun heterodimers and Jun homodimers are opposite. In contrast, X-ray crystallographic analysis, restriction fragment cycliza-

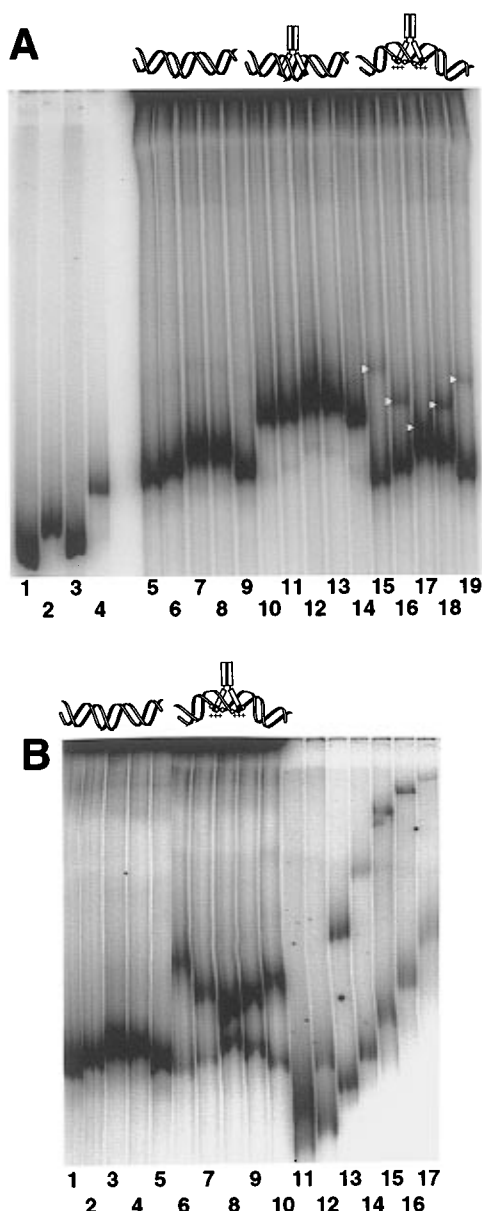


FIGURE 5: Electrophoretic mobility shift assay of GCN4, GCN4(PAA→KRR), and GCN4(PAA→KKK) homodimers bound to phasing analysis probes. (A) Lanes 1–4 contain bending standards. Lanes 1 and 2 contain circularly permuted pJT170-2 DNA fragments, where the phased array of A<sub>6</sub> tracts is located at the end or center of the fragment, respectively; lanes 3 and 4 contain circularly permuted pJT170-3 DNA as stated above for pJT170-2. Lanes 5–9 contain phasing probes from plasmids pDP-AP-1-21, -23, -26, -28, -30, respectively, incubated with an extract of *E. coli* cells containing the expression vector alone. Lanes 10–19 contain phasing probes incubated with *E. coli* extracts containing wild-type GCN4 homodimers (lanes 10–14) or GCN4(PAA→KRR) homodimers (lanes 15–19). Shifted complexes in lanes 15–19 are indicated by white triangles. (B) Lanes 1–5 contain phasing probes incubated with an extract of *E. coli* cells containing the expression vector alone. Lanes 6–10 contain phasing probes incubated with *E. coli* extracts containing GCN4(PAA→KKK) homodimers. Lanes 11–17 contain bending standards (in this case all lanes contain two circularly permuted pJT170 DNA fragments, wherein the phased A<sub>6</sub> tracts are located at the end or center of the fragment; lanes 11–17 contain pJT170-2, pJT170-3, pJT170-5, pJT170-6, pJT170-7, pJT170-8, and pJT170-9, respectively). Interpretation of the bending data is indicated schematically above the gel images.

tion, and phase-sensitive detection experiments suggest little or no DNA bending in the complexes (Glover & Harrison, 1995; Sitlani & Crothers, 1996). With respect to electro-

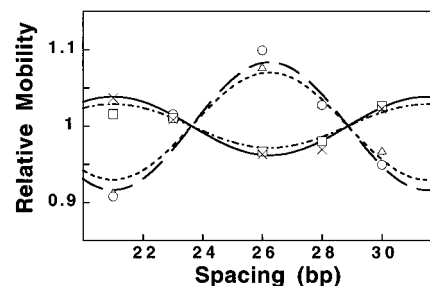


FIGURE 6: Analysis of phasing data. Relative gel mobilities are plotted as a function of the spacing (bp) between the center of the AP-1 site and the center of the A<sub>5</sub> tract array. Data were calculated as described in Experimental Procedures. Mobilities of free probes (x, solid line), wild-type GCN4-DNA complexes (□, dotted-dashed line), GCN4(PAA→KRR)-DNA complexes (○, dashed line), and GCN4(PAA→KKK)-DNA complexes (△, dotted line) reflect the average of at least two experiments. Both plots depict the calculated best fits of the data to the phasing equation described in Experimental Procedures.

Table 2: DNA Bending by GCN4 Derivatives

complex	bend angle <sup>a</sup> (deg)
probe (intrinsic curvature)	7 ± 1.0
probe + GCN4	5 ± 0.8
probe + GCN4(PAA→KRR)	−15 ± 1.3
probe + GCN4(PAA→KKK)	−14 ± 1.4

<sup>a</sup> Based on best fits to the phasing equation. Convention: bend angle >0° for bending toward the DNA major groove; bend angle <0° for bending toward the DNA minor groove. Data are based on two to four experiments.

phoretic techniques, phasing analysis and phase-sensitive detection have important differences. Phase-sensitive detection employs DNA probes with wide spacing between two bends together with short flanking sequences. This arrangement can generate complex DNA shapes, resulting in reduced, or even undetectable, electrophoretic mobility differences. In contrast, phasing analysis employs DNA probes with close spacing between two bends and long flanking sequences. This arrangement produces DNA shapes that approximate a continuous DNA bend, resulting in large mobility differences between in-phase and out-of-phase constructs. A thorough study by Kerppola (1996) clarifies the effects of probe geometry on the detection of protein-induced DNA bending. On the basis of these results, we believe that phasing analysis with the AP-1 phasing probes and homologous GCN4 derivatives we describe provides for sensitive and accurate detection of DNA bending due to electrostatic effects.

Another issue in phasing analysis is whether gel mobility of bZIP–DNA complexes can be significantly affected by the extended shapes of these proteins. It has also been hypothesized that rigid protein domains, such as the leucine zipper, may induce anomalous electrophoretic mobility (McCormick et al., 1996). These potential complications are lessened in our experiments due to utilization of truncated recombinant peptides. Moreover, the zipper region is never altered in our studies, such that changes in apparent DNA bending must be attributed to the small number of amino acid substitutions proximal to the basic region.

It has been hypothesized that electrostatic interactions (Manning et al., 1989; Mirzabekov & Rich, 1979; Strauss & Maher, 1994) might explain the different degrees of DNA bending observed for different bZIP proteins (Kerppola &

Curran, 1995). Unfortunately, the absence of DNA bending in cocrystals with bZIP proteins prevents a high-resolution analysis of the DNA bending observed in solution. However, X-ray data for the Jun-Fos heterodimer and the GCN4 homodimer complexed to duplex DNA provide many details of the protein/DNA interface (Ellenberger et al., 1992; Glover & Harrison, 1995). The central G•C base pair of the AP-1 site is recognized by a specific arginine residue (GCN4, R243; Jun, R279; Fos, R155), and this interaction is essential for high-affinity binding. Other interactions comprise an ensemble of hydrogen bonds and van der Waals contacts between the basic region of the protein and the base pairs of the AP-1 site. Which of these interactions is important for DNA bending?

Using GCN4 as a model, we report that conversion of three neutral amino acids of GCN4 to their cationic counterparts [KRR (present in Fos) or to KKK] converts GCN4 into a DNA bending protein. The resulting DNA bend has the same orientation as that attributed to Fos, i.e., compression of the minor groove such that the DNA bends away from the zipper domain. This result strongly suggests a role for electrostatic interactions in DNA bending by bZIP proteins.

Previous work in our laboratory has shown that DNA bending is induced when duplex DNA is asymmetrically neutralized by methylphosphonate substitutions or tethered cations (Strauss & Maher, 1994; Strauss et al., 1996a,b). The resulting asymmetric charge distribution causes DNA to collapse toward the neutralized face. It is intriguing to speculate that this effect contributes to DNA bending when the GCN4(PAA→KRR) or GCN4(PAA→KKK) dimers bind to the AP-1 site. Perhaps the added positive charges neutralize local phosphate diester anions resulting in an unbalanced charge on the DNA. The observed collapse of the DNA toward the neutralized surface (away from the zipper domain) is consistent with this reasoning.

Possible sites of phosphate neutralization by GCN4-(PAA→KRR) or GCN4(PAA→KKK) are at or near the phosphates highlighted on the AP-1 sequence (Figure 1). These sites were identified with reference to the crystal structure of GCN4 bound to the AP-1 site (Ellenberger et al., 1992). When mapped onto the AP-1 site, these phosphates (indicated by filled circles) are

5'-A T G A C T•C A T

3'-T A C•T G A G T A

It is important to note that the GCN4 bZIP domains contain many conserved basic residues besides the three that have been added in our study. Why does the AP-1 DNA not bend in response to conserved basic residues of GCN4? One possibility is that the cationic core of the GCN4 basic region wraps around the DNA with dyad symmetry, packing into the major groove in a manner that immobilizes the DNA such that electrostatic effects on DNA shape are not evident. In contrast, DNA proximal to the basic region (near the added cationic amino acid residues in this study) may be more flexible and able to respond to asymmetric phosphate neutralization.

Although electrostatic effects are clearly implied in this DNA bending study, it is important to note that partitioning the bending force between (i) electrostatic attraction between DNA phosphates and protein side chains vs (ii) DNA collapse due to asymmetric charge neutralization is not

possible on the basis of the present experiments. We suggest that discrimination between these kinds of bending forces can only be accomplished by "phantom protein" studies (Strauss & Maher, 1994; Strauss et al., 1996a,b) in which the degree of DNA collapse due to phosphate neutralization is measured in the absence of protein using DNA analogs designed to simulate the electrostatic consequences of protein binding. Analyses of this type may be useful to clarify the source of DNA bending energy in the present experiments.

As is evident from Figure 5, crude bacterial extracts containing the GCN4(PAA→KRR) or GCN4(PAA→KKK) mutants contained reduced DNA binding activity relative to the wild-type GCN4 derivatives. Western analysis has shown that this is largely due to reduced protein expression of both mutants. In this regard, it is notable that protein expression from extracts containing a GCN4(PAA→RRR) mutant was undetectable (data not shown). However, the GCN4(PAA→KKK) mutant was expressed at higher levels and causes DNA bending identical to the GCN4(PAA→KRR) mutant.

In addition, data obtained with disulfide-linked synthetic basic regions (not shown) suggest that GCN4(PAA→KRR) has a lower binding affinity compared to wild-type GCN4 derivatives. This reduced affinity might relate to the high local charge predicted for such a complex, but the same local pattern of basic residues is not uncommon among bZIP heterodimers (e.g., Fos-ATF-2) that stably bind to duplex DNA. Thus the origin of decreased DNA binding affinity for this particular mutant remains obscure.

The present data contribute to the view that some examples of DNA bending by proteins may be understood in terms of DNA collapse due to asymmetric phosphate neutralization by cationic amino acids. These forces may explain some of the DNA bending in the nucleosome (Crothers, 1994) and have been plausibly extended to site-specific DNA bending proteins such as PU.1 (Kodandapani et al., 1996; Pio et al., 1996) and bZIP homodimers (this work). Together with different bending mechanisms thought to be involved in other DNA bending molecules (e.g., LEF-1, SRY, HMG, and TBP; Werner et al., 1996), the forces involved in configuring nucleoprotein complexes may soon be better appreciated.

## NOTE ADDED IN PROOF

Similar effects of cationic amino acid substitutions on apparent bending of the AP-1 site have recently been reported for the bZIP domains of Jun and Fos (Leonard et al., 1997; Paolella et al., 1997).

## ACKNOWLEDGMENT

We thank B. Mueller-Hill for plasmid pPLc28-bZIP, T. Kerppola for pJT170 plasmids, and A. Schepartz and D. Paolella for pDP-AP-1 plasmids. C. Vinson and T. Kerppola provided helpful discussions and advice, J. Vockley and W. Mohsen provided assistance with molecular graphics, and the staff of the Mayo Foundation Molecular Biology Core Facilities provided excellent oligonucleotide synthesis and DNA sequencing services.

## REFERENCES

- Bracco, L., Kotlarz, D., Kolb, A., Diekmann, S., & Buc, H. (1989) *EMBO J.* 8, 4289–4296.
- Crothers, D. M. (1994) *Science* 266, 1819–1820.

- Deen, K. C., Landers, T. A., & Berninger, M. (1983) *Anal. Biochem.* 135, 456–465.
- Ellenberger, T. E., Brandl, C. J., Struhl, K., & Harrison, S. C. (1992) *Cell* 71, 1223–1237.
- Gartenberg, M. R., & Crothers, D. M. (1988) *Nature* 333, 824–829.
- Gartenberg, M. R., & Crothers, D. M. (1991) *J. Mol. Biol.* 219, 217–230.
- Gartenberg, M. R., Ampe, C., Steitz, T. A., & Crothers, D. M. (1990) *Proc. Natl. Acad. Sci. U.S.A.* 87, 6034–6038.
- Giese, K., Kingsley, C., Kirshner, J. R., & Grosschedl, R. (1995) *Genes Dev.* 9, 995–1008.
- Glover, J. N. M., & Harrison, S. C. (1995) *Nature* 373, 257–261.
- Hagerman, P. J. (1996) *Proc. Natl. Acad. Sci. U.S.A.* 93, 9993–9996.
- Kerppola, T. K. (1994) in *Transcription: Mechanisms and Regulation* (Conaway, R. C., & Conaway, J. W., Eds.) Raven Press, Ltd., New York.
- Kerppola, T. K. (1996) *Proc. Natl. Acad. Sci. U.S.A.* 93, 10117–10112.
- Kerppola, T. K., & Curran, T. (1991a) *Science* 254, 1210–1214.
- Kerppola, T. K., & Curran, T. (1991b) *Cell* 66, 317–326.
- Kerppola, T. K., & Curran, T. (1993) *Mol. Cell. Biol.* 13, 5479–5489.
- Kerppola, T. K., & Curran, T. (1995) *Nature* 373, 199–200.
- Kim, J. L., Nikilov, D. B., & Burley, S. K. (1993a) *Nature* 365, 520.
- Kim, Y., Greiger, J. H., Hahn, S., & Sigler, P. B. (1993b) *Nature* 365, 512.
- Kodandapani, R., Pio, F., Ni, C.-Z., Piccialli, G., Klemsz, M., McKercher, S., Maki, R. A., & Ely, K. R. (1996) *Nature* 380, 456–460.
- Landschulz, W. H., Johnson, P. F., & McKnight, S. L. (1988) *Science* 240, 1759.
- Leonard, D. A., Rajaram, N., & Kerppola, T. K. (1997) *Proc. Natl. Acad. Sci. U.S.A.* 94, 4913–4918.
- Manning, G., Ebraldise, K. K., Mirzabekov, A. D., & Rich, A. (1989) *J. Biomol. Struct. Dyn.* 6, 877–889.
- McAllister, C. F., & Achberger, E. C. (1989) *J. Biol. Chem.* 264, 10451–10456.
- McCormick, R. J., Badalian, T., & Fisher, D. E. (1996) *Proc. Natl. Acad. Sci. U.S.A.* 93, 14434–14439.
- McKnight, S. L. (1991) *Sci. Am.* 264, 54–64.
- Mirzabekov, A. D., & Rich, A. (1979) *Proc. Natl. Acad. Sci. U.S.A.* 76, 1118.
- O'Neil, K. T., Shuman, J. D., Ampe, C., & DeGrado, W. F. (1991) *Biochemistry* 30, 9030–9034.
- Paolella, D. N., Palmer, C. R., & Schepartz, A. (1994) *Science* 264, 1130–1133.
- Paolella, D. N., Liu, Y., Fabian, M. A., & Schepartz, A. (1997) *Biochemistry* 36, 10033–10038.
- Parkhurst, K. M., Brenowitz, M., & Parkhurst, L. J. (1996) *Biochemistry* 35, 7459–7465.
- Perez-Martin, J., & Espinosa, M. (1993) *Science* 260, 805–807.
- Perez-Martin, J., Rojo, F., & de Lorenzo, V. (1994) *Microbiol. Rev.* 58, 268–290.
- Pio, F., Kodandapani, R., Ni, C.-Z., Shepard, W., Klemsz, M., McKercher, S., Maki, R. A., & Ely, K. R. (1996) *J. Biol. Chem.* 271, 23329–23337.
- Robertson, L. M., Kerppola, T. K., Vendrell, M., Luk, D., Smeyne, R. J., Bocchiaro, C., Morgan, J. I., & Curran, T. (1995) *Neuron* 14, 241–252.
- Sitlani, A., & Crothers, D. M. (1996) *Proc. Natl. Acad. Sci. U.S.A.* 93, 3248–3252.
- Starr, D. B., Hoopes, B. C., & Hawley, D. K. (1995) *J. Mol. Biol.* 250, 434–446.
- Strauss, J. K., & Maher, L. J. (1994) *Science* 266, 1829–1834.
- Strauss, J. K., Prakash, T. P., Roberts, C., Switzer, C., & Maher, L. J. (1996a) *Chem. Biol.* 3, 671–678.
- Strauss, J. K., Roberts, C., Nelson, M. G., Switzer, C., & Maher, L. J. (1996b) *Proc. Natl. Acad. Sci. U.S.A.* 93, 9515–9520.
- Studier, F. W., Rosenberg, A. H., Dunn, J. J., & Dubendorff, J. W. (1990) *Methods Enzymol.* 185, 60–89.
- Suckow, M., van Wilcken-Bergmann, B., & Mueller-Hill, B. (1993a) *Nucleic Acids Res.* 21, 2081–2086.
- Suckow, M., van Wilcken-Bergmann, B., & Mueller-Hill, B. (1993b) *EMBO J.* 12, 1193–2000.
- Thanos, D., & Maniatis, T. (1995) *Cell* 83, 1091.
- Thompson, J. F., & Landy, A. (1988) *Nucleic Acids Res.* 16, 9687–9705.
- Travers, A. A. (1992) *Curr. Opin. Struct. Biol.* 2, 71.
- Werner, M. H., Gronenborn, A. M., & Clore, G. M. (1996) *Science* 271, 778–784.
- Zinkel, S. S., & Crothers, D. M. (1987) *Nature* 328, 178–181.
- Zinkel, S. S., & Crothers, D. M. (1991) *J. Mol. Biol.* 219, 201–215.

BI970215U